

Neutron spectrum determination of p+Be reaction for 30 MeV protons using the multi-foil activation technique

Milan Stefanik^{1,2,*}, Eva Simeckova¹, Pavel Bem¹, Mitja Majerle¹, Jan Novak¹, Martin Ansorge^{1,2}, Jaromir Mrazek¹, and Jan Stursa¹

¹Nuclear Physics Institute of The Czech Academy of Sciences, p.r.i., Rez 130, Rez 250 68, Czechia

²Czech Technical University in Prague, Faculty of Nuclear Sciences and Physical Engineering, Brehova 7, Prague 115 19, Czechia

Abstract. At the NPI in Rez, the p + Be source reaction was investigated for 30 MeV proton beam and thick beryllium target. For neutron field determination of the p(30)+Be source reaction in close source-to-sample distance, the multi-foil activation technique with a set of 10 activation materials (Au, Co, Lu, Ti, In, Al, Y, Fe, Ni, Nb) was utilized. From resulting reaction rates, the neutron spectrum was reconstructed using the SAND-II unfolding code. New neutron field of white spectrum up to 28 MeV has an intensity of $8.6 \times 10^{10} \text{ cm}^{-2}\text{s}^{-1}$ close to target. The obtained neutron field extends the utilization of cyclotron-based fast neutron sources at the NPI and provides new experimental opportunities for future irradiation experiments such as fast neutron activation analysis, nuclear data validation, and radiation damage study of electronics and materials for nuclear energetics.

1 Introduction

Nowadays, many older research nuclear reactors have reached their end of life-cycle and are being gradually decommissioned. The useful replacement for them seems to be small compact accelerator-driven neutron sources. Accelerator-driven neutron sources are safe, small, and cheap solution. They can be used for isotope production, neutron activation analysis, material irradiation, sub-surface exploration, nuclear data measurements, neutron imaging, silicon transmutation, and with suitable moderator also for boron neutron capture therapy. Many compact neutron sources in the world are based on Be-targets.

2 Materials and methods

2.1 The p+Be source reaction

Proton bombardment of thick beryllium target produces the broad neutron spectrum (see Fig. 1). The high energy fraction of spectrum is formed by the ${}^9\text{Be}(p,n){}^9\text{B}$ reaction with a Q -value of -1.85 MeV [1]. General neutron continuum and low energy region of spectrum are caused by the multi-body break-up processes ${}^9\text{Be}(p,pn){}^8\text{Be}$, ${}^9\text{Be}(p,\alpha){}^5\text{He}^*$, ${}^9\text{Be}(p,\alpha n){}^5\text{Li}$, ${}^9\text{Be}(p,p\alpha n){}^4\text{He}$ with negative Q -values [1]. Neutron mean energy of p+Be spectrum above 2 MeV is given by relation $\bar{E}_n = 0.47 \cdot E_p - 2.2$, where E_p represents the proton energy [2–4]. The p+Be interaction was earlier studied by several scientists [4–10].

2.2 Neutron source NG-2 with beryllium target

The NPI CAS in Rez operates the cyclotron based neutron source NG-2 with thick beryllium target [11]. The target

*e-mail: milan.stefanik@jfifi.cvut.cz

station uses 8 mm thick beryllium target with a diameter of 50 mm. Beryllium target is cooled on the back side by 5 mm thick layer of flowing alcohol; charged particle currents on target and collimators are monitored on-line. The neutron source is standardly operated with 35 MeV proton beam which provides broad spectrum up to 33 MeV with fast neutron flux of $10^{10} \text{ cm}^{-2}\text{s}^{-1}$ [12].

To extend the utilization of the NG-2 neutron source, the neutron fields for various energies of proton or deuteron beams need to be studied. In this manner, the new neutron field based on 30 MeV protons on Be-layer was recently investigated and is described in this paper.

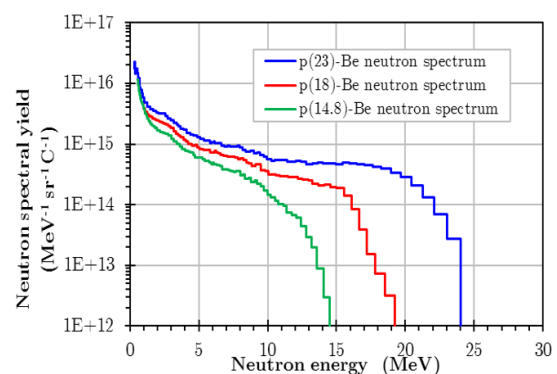


Figure 1. The p+Be neutron spectra measured by M.A. Lone using time-of-flight technique. [4]

2.3 Multi-foil activation technique

The multi-foil activation technique is the off-line neutron spectrometry method that allows the measurement of in-

tensive neutron field in experimental arrangements, where the dimensions of neutron source and activation detectors and their distance are comparable. Other techniques are not easily usable under these conditions. The neutron activation technique uses the stack of spectrometric thin foils consisting of materials that are sensitive to various energy regions of neutron spectrum depending on the character of activation cross-sections $\sigma_i(E_n)$. Foil stack is activated by neutrons at chosen position in neutron field; the radioactive nuclei are produced in foils by the activation and threshold reactions. Subsequently, the activated foils are investigated by nuclear gamma-ray spectrometry using the precise semiconductor HPGe detector. And the reaction rates per one target nucleus R_{R_i} , that represent the responses of activation foils to the neutron field, are determined. From measured reaction rates, the neutron spectrum $\phi(E_n)$ is reconstructed using the deconvolution code. The above described experimental technique is used for measurement of neutron fields with broad spectrum.

At the NPI, the multi-foil activation method was used for neutron spectrum measurement of neutron generators with p(35)+Be [12, 13], d(20)+Be [14], d(15)+Be [15], and p(37)+D₂O [16] source reactions. The neutron sources are involved in fusion related research tasks [17].

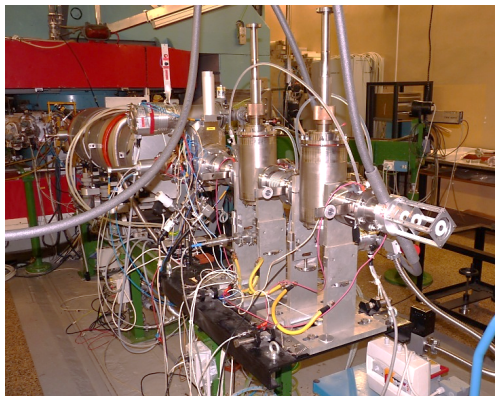


Figure 2. Beryllium target station driven by isochronous cyclotron U-120M at NPI Rez.

2.4 The p(30)+Be neutron spectrum determination

The neutron field from proton bombardment of a thick beryllium target was analysed in open space geometry by activation foil technique. The neutron energy spectra were measured at two source-to-sample distances, i.e. at a distance of 14 mm (marked as position P0) and distance of 154 mm (position P14) from source target. Sets of ten activation materials were used to measure the response to the neutron field at both main positions. The sets included Al, Au, In, Ti, Fe, Y, Lu, Co, Ni, and Nb. The longitudinal distribution of neutron flux was monitored using Au, Al, and In foils located at distances of 34 mm (position P2) and 74 mm (position P6) from Be-target.

In the experiment, the foil stacks were fixed at aluminium holder and were irradiated for 14.2 h. The beryllium target was bombarded by 30 MeV proton beam with

mean intensity of 10.9 μ A. After irradiation, the activated foils were transported to the gamma-ray laboratory. They were measured in cycle using the HPGe detector for seven weeks. In acquired gamma-ray spectra, the activation products were identified based on energy and intensity of gamma-lines and with respects to their half-lives and reaction thresholds (the observed radionuclides with their properties are listed in Tab. 1). The main output of gamma ray spectrometry were the sets of 30 reaction rates.

A modified version of SAND-II deconvolution code [18] was used to reconstruct the neutron spectra based on experimental reaction rates and corresponding activation cross-section from the EAF-2010 data library [19]. A priori information on the studied neutron spectrum, that was required by deconvolution procedure, was calculated in Monte Carlo MCNPX code [20] employing the ENDF/B-V.II [21] and LA-150h [20] data libraries.

Table 1. Activation and threshold reactions observed in irradiation experiment and successfully used for neutron spectra deconvolution. [1, 22]

Activation reaction	E_{thresh} (MeV)	$T_{1/2}$	E_{γ} (keV)	I_{γ} (%)
$^{27}\text{Al}(n,\alpha)^{24}\text{Na}$	3.3	14.9 h	1 368.6	100.0
$^{46}\text{Ti}(n,p)^{46}\text{Sc}$	1.6	83.8 d	1 120.5	99.9
$^{47}\text{Ti}(n,p)^{47}\text{Sc}$	0.0	3.4 d	159.8	68.3
$^{48}\text{Ti}(n,p)^{48}\text{Sc}$	3.3	43.7 h	1 312.1	100.0
$^{50}\text{Ti}(n,\alpha)^{47}\text{Ca}$	3.3	4.5 d	1 297.1	71.0
$^{54}\text{Fe}(n,\alpha)^{51}\text{Cr}$	0.0	27.7 d	320.1	10.0
$^{54}\text{Fe}(n,p)^{54}\text{Mn}$	3.2	312.3 d	834.9	99.9
$^{56}\text{Fe}(n,p)^{56}\text{Mn}$	2.9	2.6 h	846.8	98.9
$^{59}\text{Co}(n,\gamma)^{60}\text{Co}$	0.0	5.3 y	1 332.5	99.9
$^{59}\text{Co}(n,2n)^{58}\text{Co}$	10.5	70.9 d	810.8	99.0
$^{59}\text{Co}(n,3n)^{57}\text{Co}$	17.3	271.8 d	122.1	85.6
$^{59}\text{Co}(n,p)^{59}\text{Fe}$	1.5	44.5 d	1 099.3	56.5
$^{59}\text{Co}(n,\alpha)^{56}\text{Mn}$	1.8	2.6 h	846.8	98.9
$^{60}\text{Ni}(n,p)^{60}\text{Co}$	2.0	5.3 y	1 332.5	99.9
$^{58}\text{Ni}(n,p)^{58}\text{Co}$	1.5	70.9 d	810.8	99.0
$^{57}\text{Ni}(n,p)^{57}\text{Co}$	5.8	271.8 d	122.1	85.6
$^{58}\text{Ni}(n,2n)^{57}\text{Ni}$	12.2	35.6 h	1 377.6	81.7
$^{89}\text{Y}(n,\gamma)^{90\text{m}}\text{Y}$	0.0	3.2 h	202.5	97.3
$^{89}\text{Y}(n,2n)^{88}\text{Y}$	11.1	106.7 d	1 836.1	99.2
$^{93}\text{Nb}(n,\alpha)^{90\text{m}}\text{Y}$	0.0	3.2 h	202.5	97.3
$^{93}\text{Nb}(n,2n)^{92\text{m}}\text{Nb}$	9.1	10.2 d	934.5	99.0
$^{115}\text{In}(n,n')^{115\text{m}}\text{In}$	0.3	4.5 h	336.2	45.8
$^{\text{nat}}\text{Lu}(n,x)^{176\text{m}}\text{Lu}$	0.0	3.6 h	88.3	8.90
$^{\text{nat}}\text{Lu}(n,x)^{173}\text{Lu}$	14.2	1.3 y	78.6	11.8
$^{\text{nat}}\text{Lu}(n,x)^{174}\text{Lu}$	7.4	3.3 y	1 241.9	5.1
$^{197}\text{Au}(n,\gamma)^{198}\text{Au}$	0.0	2.7 d	411.8	96.0
$^{197}\text{Au}(n,2n)^{196}\text{Au}$	8.2	6.2 d	355.7	87.0
$\text{Au}(n,2n)^{196\text{m}2}\text{Au}$	8.2	9.6 h	147.8	43.0
$^{197}\text{Au}(n,3n)^{195}\text{Au}$	14.6	186.1 d	98.9	10.9
$^{197}\text{Au}(n,4n)^{194}\text{Au}$	23.2	38.0 h	293.6	10.4

2.5 Results and discussions

The SAND-II reconstructed neutron energy spectra of the p(30)+Be source for both irradiation positions (position

P0 and P14) are depicted in Fig. 3; the MCNPX predictions are also included in the graph, and they are in good agreement with experimental spectra. In Fig. 4, the resulting spectra are displayed in logarithmic energy scale.

The quality of obtained neutron spectra was checked using the following tests. The mean energy of determined neutron field is 11.9 MeV and is identical to predictions based on Lone equation [4]. The ratios of reaction rates calculated based on unfolded spectra and cross-section data from EAF-2010 library to experimentally measured reaction rates are close to unity (see Fig. 5). And as it can be seen from Fig. 6, the ratios of experimental reaction rates from position P0 to P14 agrees really well with ratios of reconstructed spectral distribution at position P0 to P14. All these facts have confirmed the correctness of unfolded spectra based on SAND-II optimisation process. Moreover, the longitudinal distribution of neutron flux in dependence on target-to-sample distance is shown in Fig. 7

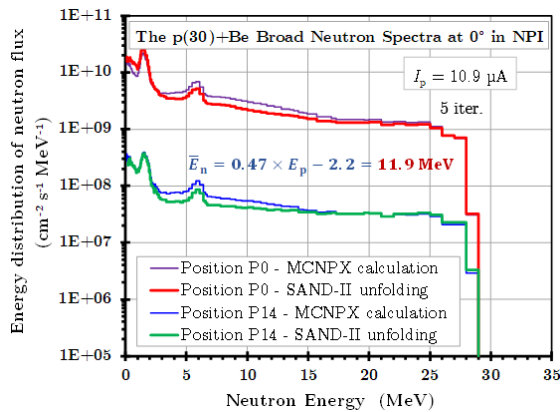


Figure 3. Novel p(30)+Be neutron spectra of NG-2 generator at two irradiation positions measured using multi-foil activation technique at NPI.

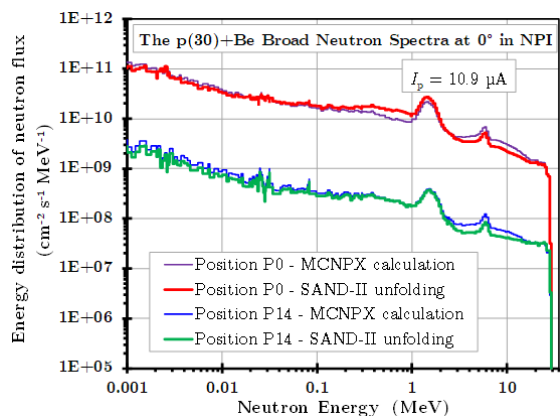


Figure 4. Novel p(30)+Be neutron energy spectra of NG-2 generator at NPI in log-log scale.

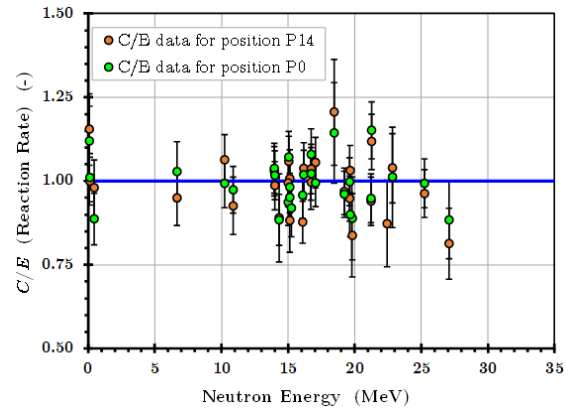


Figure 5. Calculated-to-experimental reaction rates ratios for investigated positions P0 and P14.

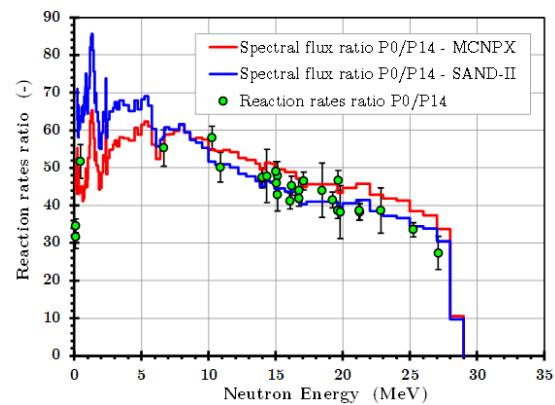


Figure 6. Reaction rates ratios and neutron spectral distribution ratios.

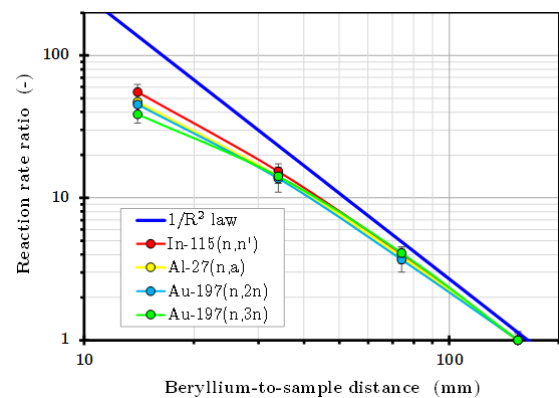


Figure 7. Reaction rates ratios in dependence on target-to-sample distance.

3 Conclusions

The brand new neutron field based on p+Be interaction for 30 MeV proton beam with 10.9 μA intensity was recently developed at the NPI Rez. The thick-target broad neutron spectra have the energy range up to 28 MeV with mean energy of 11.9 MeV. The shape of the obtained neutron spectra agrees well with the results for p+Be sources by other

Table 2. Calculated-to-experimental reaction rates ratios for deconvoluted neutron energy spectra.

Activation reaction	Position P0	Position P14
$^{27}\text{Al}(n,\alpha)^{24}\text{Na}$	1.04 ± 0.07	1.03 ± 0.07
$^{46}\text{Ti}(n,p)^{46}\text{Sc}$	1.02 ± 0.08	1.00 ± 0.08
$^{47}\text{Ti}(n,p)^{47}\text{Sc}$	1.15 ± 0.09	1.11 ± 0.08
$^{48}\text{Ti}(n,p)^{48}\text{Sc}$	0.99 ± 0.07	1.05 ± 0.07
$^{50}\text{Ti}(n,\alpha)^{47}\text{Ca}$	0.89 ± 0.12	0.84 ± 0.12
$^{54}\text{Fe}(n,\alpha)^{51}\text{Cr}$	0.95 ± 0.07	0.88 ± 0.09
$^{54}\text{Fe}(n,p)^{54}\text{Mn}$	1.01 ± 0.06	0.99 ± 0.07
$^{56}\text{Fe}(n,p)^{56}\text{Mn}$	1.07 ± 0.08	1.06 ± 0.08
$^{59}\text{Co}(n,\gamma)^{60}\text{Co}$	1.12 ± 0.10	1.15 ± 0.11
$^{59}\text{Co}(n,2n)^{58}\text{Co}$	0.96 ± 0.06	0.97 ± 0.07
$^{59}\text{Co}(n,3n)^{57}\text{Co}$	0.99 ± 0.07	0.96 ± 0.07
$^{59}\text{Co}(n,p)^{59}\text{Fe}$	0.98 ± 0.08	1.00 ± 0.09
$^{59}\text{Co}(n,\alpha)^{56}\text{Mn}$	0.94 ± 0.06	0.99 ± 0.07
$^{60}\text{Ni}(n,p)^{60}\text{Co}$	0.88 ± 0.08	0.89 ± 0.13
$^{58}\text{Ni}(n,p)^{58}\text{Co}$	0.99 ± 0.07	1.06 ± 0.08
$^{57}\text{Ni}(n,p)^{57}\text{Co}$	0.90 ± 0.06	1.03 ± 0.07
$^{58}\text{Ni}(n,2n)^{57}\text{Ni}$	0.95 ± 0.07	0.94 ± 0.07
$^{89}\text{Y}(n,\gamma)^{90m}\text{Y}$	0.97 ± 0.07	0.93 ± 0.08
$^{89}\text{Y}(n,2n)^{88}\text{Y}$	1.00 ± 0.06	0.95 ± 0.07
$^{93}\text{Nb}(n,\alpha)^{90m}\text{Y}$	0.96 ± 0.06	0.88 ± 0.06
$^{93}\text{Nb}(n,2n)^{92m}\text{Nb}$	1.07 ± 0.08	1.03 ± 0.07
$^{115}\text{In}(n,n')^{115m}\text{In}$	1.02 ± 0.09	0.95 ± 0.08
$^{\text{nat}}\text{Lu}(n,x)^{176m}\text{Lu}$	0.89 ± 0.08	0.98 ± 0.09
$^{\text{nat}}\text{Lu}(n,x)^{173}\text{Lu}$	–	0.87 ± 0.13
$^{\text{nat}}\text{Lu}(n,x)^{174}\text{Lu}$	0.92 ± 0.09	–
$^{197}\text{Au}(n,\gamma)^{198}\text{Au}$	1.01 ± 0.07	1.00 ± 0.07
$^{197}\text{Au}(n,2n)^{196}\text{Au}$	1.02 ± 0.07	1.04 ± 0.08
$^{197}\text{Au}(n,2n)^{196m2}\text{Au}$	1.14 ± 0.14	1.20 ± 0.16
$^{197}\text{Au}(n,3n)^{195}\text{Au}$	1.01 ± 0.15	1.04 ± 0.10
$^{197}\text{Au}(n,4n)^{194}\text{Au}$	0.88 ± 0.11	0.81 ± 0.10

authors [4, 5, 8]. In open space geometry, the fast neutron spectral yield of p(30)+Be source is up to $(8.6 \pm 0.6) \times 10^{10} \text{ cm}^{-2}\text{s}^{-1}$ at position P0 and $(1.5 \pm 0.1) \times 10^9 \text{ cm}^{-2}\text{s}^{-1}$ at position P14.

This novel neutron field extends the utilization of cyclotron-based neutron sources at the NPI, and it is intended for selected applications of fast neutron activation analysis, material research, and integral validation of activation cross-sections for fusion relevant technologies. It is compatible with the main energy range of planned IFMIF-DONES facility [23].

Another important fact is that this was a study of a less explored p+Be source reaction, and new spectral information for energy range with lack of empirical data (region above 20 MeV) were obtained.

Acknowledgements

This publication was supported by OP RDE, MEYS, Czech Republic under the project CANAM, CZ.02.1.01/0.0/0.0/16_003/0001812 and project SPIRAL2-CZ, CZ.02.1.01/0.0/0.0/16_013/0001679.

This research work has also been carried out within the ADAR project. Authors gratefully acknowledge financial support from the Ministry of Education, Youth and Sports of the Czech Republic under INTER-ACTION research programme (project No. LTAUSA18198).

References

- [1] National Nuclear Data Center, Q-value Calculator [Online] (May 2019), <https://www.nndc.bnl.gov/qcalc>
- [2] A. Allisy et al., *Clinical neutron dosimetry Part I: Determination of absorbed dose in a patient treated by external beams of fast neutrons*, (ICRU Report 45, Maryland, 1989)
- [3] S. Cierjacks, *Neutron Source for Basic Physics and Applications*, (Oxford Pergamon Press, Oxford, 1983)
- [4] M.A. Lone et al., *Nucl. Instr. Meth.* **143**, p. 331–344 (1977)
- [5] H.J. Brede et al., *Nucl. Instr. Meth.* **274**, p. 332–344 (1989)
- [6] R.G. Graves et al., *Med. Phys.* **6**, p. 123–128 (1970)
- [7] F.M. Waterman et al., *Med. Phys.* **6**, p. 432–435 (1979)
- [8] W.B. Howard et al., *Nucl. Sci. Eng.* **138**, p. 145–160 (2001)
- [9] J.L. Ullman et al., *Med. Phys.* **8**, p. 396–397 (1981)
- [10] S.W. Johnsen, *Phys. Med. Biol.* **23**, p. 499–502 (1978)
- [11] Center of Accelerators and Nuclear Analytical Methods (CANAM) [Online] (May 2019), <http://canam.ujf.cas.cz>
- [12] M. Stefanik et al., *Radiat. Phys. Chem.* **155**, p. 294–298 (2019)
- [13] M. Stefanik et al., *Nucl. Data Sheets* **119**, p. 422–424 (2014)
- [14] M. Stefanik et al., *Radiat. Phys. Chem.* **140**, p. 466–477 (2017)
- [15] M. Stefanik et al., *Radiat. Phys. Chem.* **160**, p. 30–34 (2019)
- [16] S. Simakov et al., *Determination of Neutron Spectrum by the Dosimetry Foil Method up to 37 MeV, Reactor Dosimetry State of the Art 2008, Proceedings of the 13th International Symposium, Netherlands (2008)*
- [17] U. Mollendorf et al., *A nuclear simulation experiment for the International Fusion Materials Irradiation Facility (IFMIF), Karlsruhe (2002)*
- [18] SAND-II-SNL, PSR-345, UKAEA FUS (1996)
- [19] R.A. Forrest et al., EAF-2010, UKAEA FUS (2010)
- [20] L.S. Waters et al., MCNPX Users Manual V. 2.1.5
- [21] M. Chadwick et al., *Nuc. Data Sheets* **112**, 2887 (2011)
- [22] S.Y.F. Chu, *Lund/LBNL Nuclear Data Search Version 2.0* [Online] (May 2019)
- [23] A. Ibarra et al., *Nucl. Fusion* **58**, 105002 (2018)